Free Radical Scavenging by Natural Polyphenols: Atom versus Electron Transfer

ARTICLE *in* THE JOURNAL OF PHYSICAL CHEMISTRY A · MARCH 2013

Impact Factor: 2.69 · DOI: 10.1021/jp3116319 · Source: PubMed

THE JOURNAL OF PHYSICAL CHEMISTRY A

Article

pubs.acs.org/JPCA

Free Radical Scavenging by Natural Polyphenols: Atom versus Electron Transfer

Florent Di Meo,[†] Vincent Lemaur,[‡] Jérôme Cornil,[‡] Roberto Lazzaroni,[‡] Jean-Luc Duroux,[†] Yoann Olivier,[‡] and Patrick Trouillas*[,†,‡,§]

[†]Laboratoire de Chimie des Substances Naturelles EA-1069, Faculté de Pharmacie, Université de Limoges, 2 rue du Docteur Marcland, Limoges CEDEX, France

[‡]Service de Chimie des Matériaux Nouveaux, Université de Mons - UMONS, Place du Parc 20, 7000 Mons, Belgium

[§]Regional Center of Advanced Technologies and Materials, Department of Physical Chemistry, Faculty of Science, Palacký University, 17. listopadu 1192/12, 77146 Olomouc, Czech Republic

Supporting Information

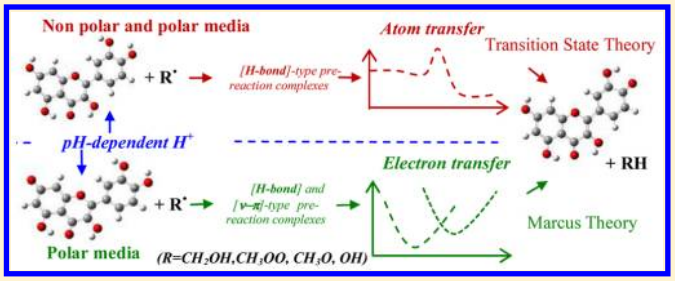

ABSTRACT: Polyphenols (synthetically modified or directly provided by human diet) scavenge free radicals by H-atom transfer and may thus decrease noxious effects due to oxidative stress. Free radical scavenging by polyphenols has been widely theoretically studied from the thermodynamic point of view whereas the kinetic point of view has been much less addressed. The present study describes kinetic-based structure−activity relationship for quercetin. This compound is very characteristic of the wide flavonoid subclass of polyphenols. H-atom transfer is a mechanism based on either atom or electron transfer. This is analyzed here by quantum chemical calculations, which support the knowledge acquired from experimental studies. The competition between the different processes is discussed in terms of the nature of the prereaction complexes, the pH, the formation of activated-deprotonated forms, and the atom- and electron-transfer efficiency. The role of the catechol moiety and the 3-OH group of quercetin as scavengers of different types of free radicals ($CH_3OO^{\bullet}$, $CH_3O^{\bullet}$, $^{\bullet}OH$, and $^{\bullet}CH_2OH$) is rationalized. Identifying the exact mechanism and accurately evaluating kinetics is of fundamental importance to understand antioxidant behavior in physiological environments.

1. INTRODUCTION

Oxidative stress is ubiquitous in the human organism where it can induce various diseases, e.g., atherosclerosis,[1] inflammation,[2] Alzheimer disease,[3] lung diseases,[4] liver diseases,[5,6] and cancer.[7] It results from an imbalance between the production of reactive oxygen species (ROS), mainly free radicals, and protective effects (inhibition of free radical production, direct free radical scavenging or detoxification). Free radicals are produced by endogenous (e.g., production of $O_2^{\bullet-}$, which is rapidly transformed into other reactive oxygen species like hydrogen peroxide and $^{\bullet}OH$ radicals in the presence of metal ions) or exogenous (ionizing radiations, UV light, or pollution) processes. Different cascades of events like the oxidation of lipids (LH) in cell membranes produce a huge variety of free radical species including carbon-centered ($R^{\bullet}$ and $L^{\bullet}$), alkoxyl ($RO^{\bullet}$ and $LO^{\bullet}$), and peroxyl ($ROO^{\bullet}$ and $LOO^{\bullet}$) radicals. These free radicals can act on DNA, proteins, and lipids, in both polar and nonpolar compartments.

Antioxidant molecular systems are endogenous (e.g., catalase and glutathione peroxidase) or are provided exogenously (e.g., vitamins and polyphenols largely found in human diets, i.e., fruit, vegetables, spices, and beverages made from plants such as tea, wine, beer, infusions, fruit juices, and food supplements). Polyphenols (ArOH) are divided in various subclasses including phenolic acids, lignans, flavonoids, and tannins. The large variety of their chemical structures allows for a wide range of biological (including antioxidant) activities.[8,9]

Flavonoid derivatives (natural, metabolized, or hemisynthetic) are a large subclass of polyphenols. They are powerful free radical scavengers acting by H-atom transfer from their OH groups to the free radicals ($R^{\bullet}$):

$$ArOH + R^{\bullet} \rightarrow ArO^{\bullet} + RH \quad (1a)$$

Received: November 26, 2012
Revised: February 14, 2013
Published: February 18, 2013

dx.doi.org/10.1021/jp3116319 | J. Phys. Chem. A 2013, 117, 2082−2092

Structure−activity relationships of their antioxidant capacity have been experimentally established over the past years and rationalized on the basis of quantum-chemical studies.[10−23] The calculated thermodynamic descriptors (e.g., O−H bond dissociation enthalpies (BDEs) and π-electron conjugation) fit perfectly with the free radical scavenging activities, particularly when calculated at the DFT (density functional theory) level using hybrid functionals. Those calculations confirm (i) the important role of the 3-OH group of the quercetin derivatives (flavonols); (ii) the important role of the 2,3 double bond and the catechol moiety in the B-ring; (iii) the passive role of the 5-OH group, because it is engaged in a strong H-bond with the keto group at C4; (iv) the minor direct role of the 7-OH group (see Figure 1a for numbering);[24] and (v) the important role of

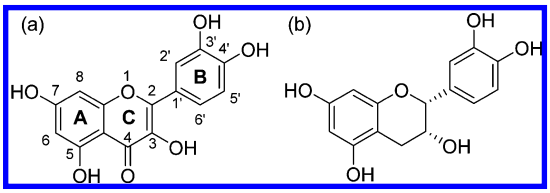

Figure 1. Chemical structures of (a) quercetin and (b) (−)-epicatechin.

intramolecular H-bonding.[10,14,25] These thermodynamic descriptors, mainly BDE, are now validated to predict the capacity of polyphenols to act as antioxidants in vitro.

However, the thermodynamic approach is not sufficient to accurately predict free radical scavenging activity in physiological environments. To be fully active, a polyphenol (or its active metabolites) must react by H-atom transfer faster than at least one of the reactions of free-radical-production cascades (e.g., the limiting propagation step in lipid peroxidation). An accurate description of the kinetics of H-atom transfer between polyphenols and free radicals is crucial to predict biological activities in vivo. Kinetic measurements (e.g., pulse radiolysis, laser flash photolysis, styrene oxidation essays) have been performed over the past years for phenol derivatives and many radicals.[22,23,26−29] The experimental exploration of antioxidant kinetics is somewhat delicate to be systematically performed for large series of compounds and under various conditions (different solvents and pH). Quantum-chemistry appears as a relevant alternative in the future to systematically evaluate such kinetic aspects. The calculated intrinsic O−H BDEs or Gibbs energies of free radical scavenging reactions provide an indirect way to estimate kinetics.[30] The rate constants can also be directly calculated. Nonetheless, to reach accuracy, the adequate theoretical methodology must be carefully chosen. A proper qualitative description would prove useful to establish structure−activity relationships in terms of kinetics. An accurate quantitative description would allow us to predict antioxidant activities in vivo.

To deal with kinetics of polyphenol free-radical-scavenging, three possible H-atom-transfer mechanisms must be considered:

(i) HAT (H-atom transfer) and PCET (proton-coupled electron transfer): HAT is somehow the pure H-atom transfer in which the proton and the electron of the H-atom are transferred to the same atomic orbital in the free radical. PCET is distinguished from the pure HAT as it involves several molecular orbitals. PCET occurs in an H-bonding prereaction complex in which the proton transfer occurs along the H-bond to one of the lone pair of the O-atom of the free radical. This transfer is coupled to the electron transfer that occurs from a lone pair of the antioxidant to the SOMO (singly occupied molecular orbital) of the free radical.[31−34] This latter mechanism is well-adapted to describe H-atom transfer from polyphenols to free radicals.[27,28,35,36] In both mechanisms, the proton and electron are transferred in one kinetic step.[37]

$$ArOH + R^{\bullet} \rightarrow ArO^{\bullet} + RH \quad (1b)$$

(ii) ET-PT (electron transfer−proton transfer) is a two-step mechanism initiated by an electron transfer (eq 2) and followed by a proton release (eq 3). PT is so fast that ET-PT can be considered as a HAT process:[38,39]

$$ArOH + R^{\bullet} \rightarrow ArOH^{\bullet+} + R^{-} \quad (2)$$

$$ArOH^{\bullet+} + R^{-} \rightarrow ArO^{\bullet} + RH \quad (3)$$

(iii) SPLET (sequential proton loss−electron transfer, eqs 4−6) is the reverse mechanism with respect to ET-PT: it is initiated by proton loss (eq 4). The polyphenol anion then undergoes an electron transfer (eq 5). SPLET is favored when the anion (ArO^{-}) is stable enough to allow electron transfer before reprotonation. This is unambiguously a three-step mechanism which is not strictly considered as HAT:[23,26,36,40]

$$ArOH \rightarrow ArO^{-} + H^{+} \quad (4)$$

$$ArO^{-} + R^{\bullet} \rightarrow ArO^{\bullet} + R^{-} \quad (5)$$

$$R^{-} + H^{+} \rightarrow RH \quad (6)$$

These three mechanisms have the same thermodynamic balance because the reactants and products are the same ($\Delta G^{PCET} = \Delta G^{ET\text{-}PT} = \Delta G^{SPLET}$). The competition between the different mechanisms is governed by the kinetics of the limiting step of each mechanism (atom transfer for PCET and electron transfer for both ET-PT and SPLET).[41]

The present work evaluates the rate constants for the antioxidant quercetin (Figure 1a), a prototypical representative of flavonoids well-adapted to tackle structure antioxidant-activity relationship. Even if it can be toxic (i.e., pro-oxidant at high concentration)[4,42] and not efficiently absorbed by the organism,[43] quercetin is widely distributed in fruit and vegetables in its glycoside form and possesses most of the chemical characteristics responsible for the free radical scavenging capacity of flavonoid-type compounds. It has extensively been studied over the past decades.

Section 2 describes the DFT-based theoretical methodology we have used; to be predictive and an efficient complementary tool of experimental data, this methodology has been carefully chosen. Section 3 describes the reaction of each OH group of quercetin with different types of free radicals (i.e., peroxyl ($ROO^{\bullet}$), hydroxyl ($^{\bullet}OH$), alkoxyl ($RO^{\bullet}$), and carbon centered ($R^{\bullet}$) radicals) produced by oxidative processes (e.g., lipid peroxidation). Flavonoids are known to act poorly as peroxyl free radical scavenger during the propagation phase of lipid peroxidation in membranes or in micelles.[44−47] They appear more efficient to scavenge free radicals during the initiation phase rather than the propagation phase. Their capacity to inhibit different sorts of free radicals is thus a key characteristic to better understand their behavior directly in living organisms. Our first goal is to provide a qualitative description, establishing

dx.doi.org/10.1021/jp3116319 | J. Phys. Chem. A 2013, 117, 2082−2092

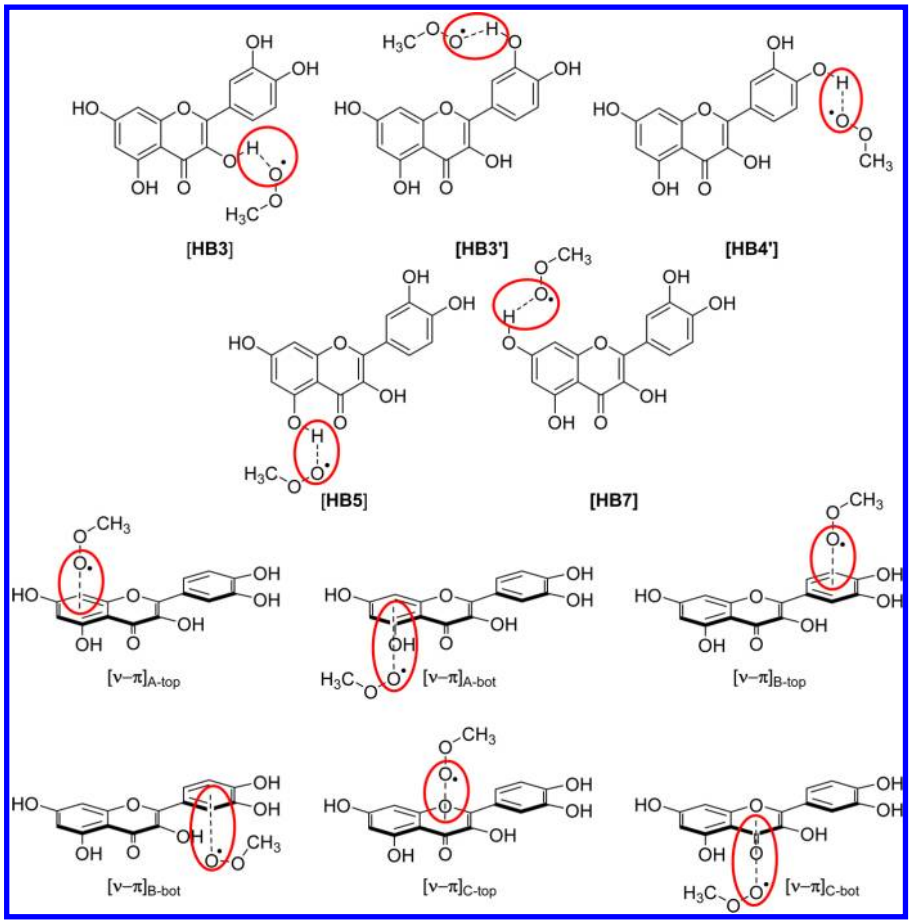

Figure 2. Structures of the different prereaction complexes with H bond ([**HB3**], [**HB3**′], [**HB4**′], [**HB5**], and [**HB7**]) and $\nu-\pi$ type interactions.

structure−activity relationships based on kinetics, complementary to thermodynamic studies. The second goal is to compare the atom and electron-transfer processes that are presented in sections 3.1 and 3.2, respectively. This requires a detailed analysis of the electronic properties of the prereaction complexes formed between quercetin and the free radicals. Concluding remarks (section 4) complete the comparison between the two processes in different environments (polar vs nonpolar).

2. THEORETICAL METHODOLOGY

2.1. Models and Methods for the Ground State. $CH_3OO^{\bullet}$, $CH_3O^{\bullet}$, and $^{\bullet}CH_2OH$ were used as prototypes for lipid (L) or small (R) peroxyl ($LOO^{\bullet}$ and $ROO^{\bullet}$), alkoxyl ($LO^{\bullet}$ and $RO^{\bullet}$), and carbon-centered ($L^{\bullet}$) radicals,[48] respectively. Flavonoid derivatives (ArOH) and their corresponding radicals ($ArO^{\bullet}$) were found to be accurately described by DFT calculations.[22,49] The B3P86 functional provides a particularly accurate evaluation of the thermodynamics of the reaction between polyphenols and free radicals.[10,50] The 6-31+G(d,p) basis set is used because it provides very similar results compared to the larger and more computationally demanding 6-311+G-(2d,3pd) basis set.[10,51] Geometries, energies including the zero-point correction (V), enthalpies (H), and Gibbs energies (G) at 298 K of the reactants and products were determined at the (U)B3P86/6-31+G(d,p) level. Ground-state geometries were confirmed by a vibrational frequency analysis that indicated the absence of imaginary frequency.

2.2. Prereaction Complexes and Description of Noncovalent Interactions. The prereaction complexes are crucial in the different mechanisms. They drive the bimolecular approach. These complexes involve noncovalent interactions (H-bonding and π-stacking interactions), which are poorly described by classical hybrid functionals. The dispersion corrected DFT-D is a successful approach to circumvent the use of high-cost post-HF methods.[52] We recently reparameterized the B3P86-D2 functional, reaching accuracy to evaluate dispersive effects in the complexation of flavonoid derivatives.[53] The geometries of the prereaction complexes were obtained with B3P86-D2 after a complete scan of possible approaches, i.e., either toward the OH groups (for the [**HBi**]-type complexes that form H-bond between the free radical and the i-OH group, Figure 2) or toward the aromatic rings (for the [$\nu-\pi$]-type complexes having noncovalent lone-pair/aromatic-ring interactions, Figure 2).

2.3. Kinetics and Transition-State Description. Concerning PCET, the transition states (TSs) were confirmed by the presence of one imaginary frequency assigned to the normal mode corresponding to the reaction studied (i.e., O−H bond cleavage and the concomitant O−H or C−H bond formation in the polyphenol and the free radical, respectively). TSs were also confirmed by the calculation of the minimum energy path (MEP) evaluated with the IRC (intrinsic reaction coordinate) algorithm as implemented in the Gaussian09 program.[54] The activation barriers were corrected by scaling factors of 0.9686 and 0.9537 for B3P86 and MPWB1K, respectively.[55]

Hybrid functionals (e.g., B3P86) are shown to underestimate the energy of the transition states (TSs) of various reactions including HAT.[55] Meta-GGA hybrid functionals such as

dx.doi.org/10.1021/jp3116319 | J. Phys. Chem. A 2013, 117, 2082−2092

Table 1. Gibbs Energy of Activation $\Delta G^{\#}_{PCET}$ (kcal mol^{-1}), Tunneling Transmission Coefficients Obtained According to the Skodje and Truhlar Formalism $\kappa(T)$, Transition Rate Constants k^{TST} and k^{PCET} (M^{-1} s^{-1}) with the B3P86 and MPWB1K Functional

	$\Delta G^{\#}_{PCET}$			κ^{TST}		k^{TST}		k^{PCET}[b]	
eq	B3P86	MPWB1K	CCSD(T)[a]	B3P86	MPWB1K	B3P86	MPWB1K	B3P86	MPWB1K
7	14.9	22.7	25.1	1	2.75×10^{3}	7.6×10^{1}	1.5×10^{-4}	7.6×10^{1}	4.1×10^{-1}
8	23.5	29.5	30.4	4.46	5.81×10^{1}	3.8×10^{-5}	1.6×10^{-9}	1.7×10^{-4}	9.0×10^{-8}
12[c]		15.8			8.79×10^{1}		1.6×10^{1}		1.4×10^{3}

[a]Performed on the MPWB1K geometry. [b]Following $k^{PCET} = \kappa^{TST} \times k^{TST}$. [c]In benzene.

Table 2. Gibbs Energies of Activation $\Delta G^{\#}_{PCET}$ (kcal mol^{-1}), Tunneling Transmission Coefficients Obtained According to the Skodje and Truhlar Formalism $\kappa(T)$ and Rate Constants k^{PCET} (M^{-1} s^{-1}) for PCET in (a) Nonpolar and (b) Polar Environments

		B3P86			MPWB1K		
Radical	OH group	$\Delta G^{\#}_{PCET}$	$\kappa(T)$	k^{PCET}	$\Delta G^{\#}_{PCET}$	$\kappa(T)$	k^{PCET}
			(a) Nonpolar Environment				
$CH_3OO^{\bullet}$	3-OH	15.5	4.0	1.2×10^{2}	29.6	1.4×10^{6}	1.6×10^{-3}
	3′-OH	8.5	1.0	3.8×10^{6}	19.7	6.3×10^{2}	1.5×10^{1}
	4′-OH	7.4	1.0	2.3×10^{7}	19.2	4.6×10^{2}	2.4×10^{1}
	5-OH	24.1	1.0	1.2×10^{-5}	34.7	2.1×10^{2}	1.2×10^{-12}
	7-OH	13.3	2.9	3.0×10^{3}	25.2	8.5×10^{1}	1.8×10^{-4}
			(b) Polar Environment				
$CH_3OO^{\bullet}$	3-OH	14.3	2.4	5.4×10^{2}	28.5	5.9×10^{6}	5.1×10^{-2}
	3′-OH	11.5	1.5	3.6×10^{4}	23.5	1.5×10^{3}	5.7×10^{-2}
	4′-OH	9.9	1.0	3.6×10^{5}	22.9	9.9×10^{2}	9.7×10^{-2}
	5-OH	22.3	1.2×10	3.4×10^{-3}	40.3	3.1×10^{11}	6.4×10^{-6}
	7-OH	14.1	1.1	3.3×10^{2}	26.5	7.1×10^{2}	1.6×10^{-4}

MPWB1K appear to be more accurate to reproduce $\Delta G^{\#}_{PCET}$ values.[55] Therefore, all the activation barriers involving HAT-(PCET) were evaluated at the (U)MPWB1K/6-31+G(d,p) level.[56] To validate this choice, the rate constants of HAT-(PCET) were calculated with (U)B3P86/6-31+G(d,p) and (U)MPWB1K/6-31+G(d,p) and were compared to the robust (U)CCSD(T)/cc-pVTZ//(U)MPWB1K/6-31+G(d,p) level of theory (Table 1) for the following two prototype reactions from phenol (PhOH) and propane ($CH_3-CH_2-CH_3$) to $CH_3OO^{\bullet}$:

$$PhOH + CH_3OO^{\bullet} \rightarrow PhO^{\bullet} + CH_3OOH \quad (7)$$

$$CH_3-CH_2-CH_3 + CH_3OO^{\bullet} \rightarrow CH_3-{}^{\bullet}CH-CH_3 + CH_3OOH \quad (8)$$

The free energy barriers of reaction 7 are 14.9, 22.7, and 25.1 kcal mol^{-1} with B3P86, MPWB1K, and CCSD(T), respectively; the corresponding values for reaction 8 are 23.5, 29.5, and 30.4 kcal mol^{-1} (Table 1). As expected and firmly confirmed by several theoretical works for many HAT(PCET) prototype reactions,[31,32] the free energy barriers appear underestimated with classical hybrid functionals (e.g., B3P86) whereas those obtained with MPWB1K are closer to those obtained at the CCSD(T) level. The extrapolation to larger molecular systems, in particular π-conjugated systems such as polyphenols, is delicate and will be discussed below on the basis of the present work and the related literature. In the present article, both B3P86 and MBWB1K results will be shown in Tables 1 and 2 for the sake of comparison.

2.4. Solvent Effects. Solvent effects were taken into account during optimization implicitly by a PCM (polarizable continuum model) method. The IEFPCM (integral equation formalism PCM) method coupled to UA0 radii was used.[57,58] The PCET, ET-PT, and SPLET mechanisms have been studied in media corresponding to benzene ($\varepsilon = 2.27$) and water ($\varepsilon = 78.35$). The former solvent simulates the behavior in nonpolar environments (e.g., lipid bilayer membranes) and the latter describes the behavior in polar environments. All calculations were carried out using Gaussian09[54] and Orca.[59]

3. RESULTS AND DISCUSSION

The free radical scavenging action is driven either by atom transfer (PCET) or by electron transfer (ET-PT and SPLET). These two physical mechanisms are treated by two different theories. The former is well-described by the transition-state theory (TST) and the corresponding refinements, whereas for the latter, Marcus theory and related formalisms offer an appropriate framework. Those three processes can take place by overcoming the free energy barrier or by tunneling along the reaction coordinate. Therefore, rate constants rather than Gibbs activation energies ($\Delta G^{\#}$) must be evaluated to compare the kinetics of these three mechanisms.

3.1. Atom-Transfer Processes (PCET). As already described, PCET occurs when [**HBi**]-type prereaction complexes are formed;[34,36,60] H-bonds are formed between the free radical and one of the OH groups of quercetin.

The rate constants of PCET were calculated within the conventional TST framework:[61,62]

$$k^{PCET} = \kappa(T)k^{TST} = \kappa(T)\frac{k_b T}{h}\exp\left(-\frac{\Delta G^{\#}_{PCET}}{RT}\right) \quad (9)$$

$\Delta G^{\#}_{PCET}$ is calculated as the difference in Gibbs energy between the TS and the reactants, $\kappa(T)$ is the transmission coefficient; k_b is the Boltzmann constant, and T is the temperature (298 K).

The $\kappa(T)$ transmission coefficient associated to quantum tunneling along the reaction coordinate was evaluated by the Skodje and Truhlar (S/T) method.[63] To describe the MEP

dx.doi.org/10.1021/jp3116319 | J. Phys. Chem. A 2013, 117, 2082−2092

Table 3. Interaction Energy ΔE_{int} (kcal mol^{-1}) within the Pre-reaction Complex, Internal λ_i and External λ_s Reorganization Energies (kcal mol^{-1}), Electronic Coupling V_{RP} (kcal mol^{-1}), Gibbs Energy of the Reaction $\Delta G°$ (kcal mol^{-1}), Rate Constants $k^{ET\text{-}PT}$ (M^{-1} s^{-1}) Including the Tunneling Transmission Coefficient κ^{LJ} Obtained within the Marcus−Levich−Jortner Formalism of the Electron-Transfer Reaction for the ET-PT Mechanism in (a) Nonpolar and (b) Polar Solvents

free radical	prereactant complex	ΔE_{int}	λ_i	λ_s	V_{RP}	$\Delta G°$	$k^{ET\text{-}PT}$
			(a) Nonpolar Solvent				
$CH_3OO^•$	[**HB3**]	−2.8	13.9	0.1	0.1	55.6	
	[**HB3′**]	−6.4	13.9	0.1	0.1	43.5	
	[**HB4′**]	−6.6	13.9	0.0	−1.8	45.1	
	[**HB5**]	−1.2	13.9	0.1	−0.2	65.6	
	[**HB7**]	−6.2	13.9	0.1	0.0	48.1	
	$[\nu-\pi]_{A\text{-}bot}$	−3.8	13.9	0.1	−1.8	56.3	
	$[\nu-\pi]_{A\text{-}top}$	−3.8	13.9	0.1	1.9	56.2	
	$[\nu-\pi]_{B\text{-}bot}$	−4.2	13.9	0.1	−1.4	56.2	
	$[\nu-\pi]_{B\text{-}top}$	−3.5	13.9	0.1	0.5	56.1	
	$[\nu-\pi]_{C\text{-}bot}$	−3.8	13.9	0.1	1.9	56.2	
	$[\nu-\pi]_{C\text{-}top}$	−4.0	13.9	0.1	2.2	56.0	
$CH_3O^•$	[**HB3**]	−2.2	7.4	0.1	−5.1	45.2	
$^•CH_2OH$	[**HB3**]	−3.4	22.8	0.1	−3.2	89.2	
			(b) Polar Solvent				
$CH_3OO^•$	[**HB3**]	−1.8	13.3	4.9	0.0	28.2	2.9×10^{-32}
	[**HB3′**]	−4.0	13.3	6.8	−0.2	27.7	6.7×10^{-22}
	[**HB4′**]	−3.6	13.3	3.4	1.6	27.8	8.2×10^{-40}
	[**HB5**]	−0.2	13.3	10.7	0.2	28.5	3.4×10^{-16}
	[**HB7**]	−3.9	13.3	11.3	−0.5	27.9	7.9×10^{-14}
	$[\nu-\pi]_{A\text{-}bot}$	−2.2	13.3	8.0	0.9	28.2	2.7×10^{-18}
	$[\nu-\pi]_{A\text{-}top}$	−2.6	13.3	8.7	−2.4	28.2	3.2×10^{-16}
	$[\nu-\pi]_{B\text{-}bot}$	0.5	13.3	2.5	0.0	28.1	5.2×10^{-59}
	$[\nu-\pi]_{B\text{-}top}$	−2.9	13.3	5.0	0.0	28.1	4.7×10^{-31}
	$[\nu-\pi]_{C\text{-}bot}$	−2.3	13.3	8.2	−1.9	28.2	2.8×10^{-17}
	$[\nu-\pi]_{C\text{-}top}$	−2.8	13.3	6.1	0.8	28.1	1.1×10^{-23}
$CH_3O^•$	[**HB3**]	−3.3	6.3	5.6	−6.2	21.0	1.6×10^{-12}
$^•CH_2OH$	[**HB3**]	−2.2	22.2	4.4	−3.2	71.9	

(minimum energy path) and tunneling, the S/T method uses the TS imaginary frequency and the height of the potential energy barrier including the zero-point correction. The transmission coefficients are given by the following expressions (eqs 10 and 11):

$-\beta < \alpha$:

$$\kappa(T) = \frac{\beta\pi/\alpha}{\sin(\beta\pi/\alpha)} - \frac{\beta}{\beta-\alpha}\exp[(\beta-\alpha)(\Delta V^{\#} - V)] \quad (10)$$

$-\beta > \alpha$:

$$\kappa(T) = \frac{\beta}{\beta-\alpha}\{\exp[(\beta-\alpha)(\Delta V^{\#} - V)] - 1\} \quad (11)$$

where $\alpha = 2\pi/(h\cdot\mathrm{Im}(\nu^{\#}))$, $\beta = 1/k_bT$, $\Delta V^{\#}$ is the zero-point-corrected potential energy difference between TS and reactants, and V is either zero (for an exoergic reaction) or the zero-point-corrected energy difference between products and reactants (for an endoergic reaction). $\nu^{\#}$ is the TS imaginary frequency.

The $\kappa(T)$ obtained is similar to those provided by CVT/SCT (canonical variational transition-state theory/small-curvature tunneling) on epicatechin[64] and quercetin,[57] as calculated with MBWB1K.

3.1.1. Reactivity of Quercetin with Peroxyl Radicals. The $CH_3OO^•$-scavenging reaction strongly depends on the OH group.[65] In the nonpolar and polar environment, the hierarchies are 4′-OH > 3′-OH > 3-OH > 7-OH ≫ 5-OH (Table 2a) and 4′-OH ∼ 3′-OH ∼ 3-OH > 7-OH ∼ 5-OH (Table 2b), respectively. These hierarchies are very consistent with the experimental knowledge, confirming the robustness of the methodology to provide an accurate qualitative description of the free radical scavenging kinetics of polyphenols. These hierarchies are similarly obtained with both functionals B3P86 and MPWB1K and with or without PCM-type solvent effects.

From the quantitative point of the view, the values obtained here with MPWB1K are relatively similar to those obtained with the few theoretical studies performed at a similar level of calculation for the 4′-OH group of epicatechin (Figure 1b, at the ONIOM(CCSD(T)/6-31G(d,p):MPWB1K/6-31G(d,p))//MPWB1K/6-31G(d,p) level within the CVT formalism)[64] and for the 4′-OH group of quercetin (with MPWB1K/6-311G-(d,p)).[60] This appears encouraging to validate the choice of this methodology to evaluate atom-transfer rates. The gas phase values of ref 60 were successfully compared to the rate constants of DPPH(2,2-diphenyl-1-picryl-hydrazyl) scavenging by quercetin, which is around 5×10^3 M^{-1} s^{-1} in methanol.[66] However, it must be stressed that the rate constants evaluated with MPWB1K in the presence of PCM-type solvent appear dramatically lowered compared to the gas phase values, i.e., 2.3×10^1 and 9.7×10^{-2} M^{-1} s^{-1} for the 4′-OH group in benzene and water, respectively (Table 2b, these results are in agreement with ref 60 for the same compound).

It is noteworthy that the rate constants of DPPH-scavenging by quercetin were also measured when favoring only the PCET mechanism (methanol in the presence of acetic acid and ethyl

dx.doi.org/10.1021/jp3116319 | J. Phys. Chem. A 2013, 117, 2082−2092

Table 4. Interaction Energy ΔE_{int} (kcal mol^{-1}) within the Pre-reaction Complex, Internal λ_i and External λ_s Reorganization Energies (kcal mol^{-1}), Electronic Coupling V_{RP} (kcal mol^{-1}), Gibbs Energy of the Reaction $\Delta G°$ (kcal mol^{-1}), Rate Constants k^{SPLET} (M^{-1} s^{-1}) Including the Tunneling Transmission Coefficient κ^{LJ} Obtained within the Marcus−Levich−Jortner Formalism of the Electron-Transfer Reaction for SPLET and Rate Constant Ratio K with Respect to the Fastest Reaction in Polar Solvent

free radical	prereactant complex	ΔE_{int}	λ_i	λ_s	V_{RP}	$\Delta G°$	k^{SPLET}	K
$CH_3OO^•$	[**HB3**]-7H+	−1.2	11.6	8.7	0.1	17.9	4.0×10^{-1}	1×10^{-12}
	[**HB3′**]-7H+	−4.0	11.6	9.4	0.1	17.5	5.5×10^{-5}	4×10^{-12}
	[**HB4′**]-7H+	−3.5	11.6	12.7	−1.3	17.5	4.0×10^{-1}	3×10^{-8}
	[**HB5**]-7H+	−3.4	11.6	4.3	−0.8	17.9	2.8×10^{-9}	2×10^{-16}
	$[\nu-\pi]_{Atop}$-7H+	−2.3	11.6	8.7	2.0	18.0	1.6×10^{-2}	1×10^{-9}
	$[\nu-\pi]_{Atop}$-7H+	−2.3	11.6	9.6	2.0	18.0	4.9×10^{-2}	4×10^{-9}
	$[\nu-\pi]_{Bbot}$-7H+	−2.8	11.6	8.3	0.4	17.9	3.4×10^{-4}	3×10^{-11}
	$[\nu-\pi]_{Btop}$-7H+	−2.2	11.6	14.0	0.5	17.9	3.6×10^{-2}	3×10^{-9}
	$[\nu-\pi]_{Cbot}$-7H+	−1.8	11.6	8.5	−1.8	18.0	1.0×10^{-2}	8×10^{-10}
	$[\nu-\pi]_{Ctop}$-7H+	−2.7	11.6	10.0	0.5	17.9	5.4×10^{-3}	4×10^{-10}
	[**HB3′**]-4′H+	−0.4	12.6	2.7	−0.1	9.2	2.7	2×10^{-7}
	[**HB7**]-4′H+	−8.9	12.6	12.9	−0.8	9.1	2.3×10^{5}	2×10^{-2}
	[**HB7**]-3H+	−3.6	13.0	10.6	−0.2	4.9	8.7×10^{6}	7×10^{-1}
	[**HB3′**]-3H+	−3.8	13.0	9.0	−0.2	4.8	1.3×10^{7}	1
$CH_3O^•$	[**HB3**]-7H+	−2.8	4.6	47.2	1.0	−1.9	2.3×10^{12}	
$^•CH_2OH$	[**HB3**]-7H+	−1.7	20.5	46.0	−0.9	49.0	1.3×10^{-52}	

acetate).[67] In this case, the rate constants were much lower (5.0×10^1 and 9.3×10^0 M^{-1} s^{-1}, respectively) than those obtained in ref 66. This would fit better with the MPWB1K rate constants. However, DPPH is much less reactive than ROO$^•$ radicals (e.g., around 10^7 M^{-1} s^{-1} for the $Ph_2CHOO^•$ scavenging by quercetin in chlorobenzene[68]) and is far from an ideal benchmark. Reaching a quantitative accuracy remains a critical and delicate issue because the rate constants can be influenced by very slight fluctuations of $\Delta G^{\#}$ and a significant underestimation of k^{PCET} is therefore suspected. This poor description of PCET rate constants has already been pointed out[31] and attributed to "a poor description of the charge separation in the PCET transition state". Although B3P86 appears to slightly enhancing the rate constants, a compensation of error is more likely, as we observed a better description of HAT activation barriers with MPWB1K (in section 2.3) in agreement with the related literature. The solvent effects also appear crucial (see Supplorting Information for an additional discussion on kinetic solvent effects, as described in the related literature).[28,69]

The major conclusion that must be drawn is that whatever the DFT functional (B3P86 and MPWB1K in this study) the PCET rate constants are underestimated but provide a reliable qualitative description (same structure activity relationship). Both sets of values are presented in Table 2 but the following discussions are based on the MPWB1K set of values, keeping in mind that, for the sake of experimental comparison, an unknown correcting factor should shift all values.

3.1.2. Reactivity of Quercetin with Other Free Radicals. The rate constants with the $CH_3O^•$ free radical are slightly higher than with $CH_3OO^•$ (k^{PCET} = 6.4×10^1 and 6.2 M^{-1} s^{-1} in the nonpolar and polar solvents, respectively, Table 2) and much smaller than with $^•OH$, due to the presence of the CH_3 group, which considerably increases the stability of the free radical, in turn decreasing its reactivity. Again, the underestimation of k^{PCET} is confirmed for alkoxy radicals. Considering the following reaction

$$PhOH + t\text{-}BuO^• \rightarrow PhO^• + t\text{-}BuOH \quad (12)$$

the MBWB1K rate constant calculated in benzene is 1.4×10^3 M^{-1} s^{-1} whereas the experimental value measured in nonpolar solvents for which PCET is the only possible mechanism, is around 10^8 M^{-1} s^{-1}.[28,36]

The rate constants with $^•CH_2OH$ are much smaller than with the $CH_3O^•$ free radicals. This is due to the fact that the PCET reaction with the carbon-centered free radical $^•CH_2OH$ implies a strong reorganization, from sp^2 to sp^3 hybridization. This reorganization requires a large activation free energy (21.1 and 23.7 kcal mol^{-1} in the nonpolar and polar solvents, respectively), which is somewhat mitigated by a sizable tunneling transmission coefficient in both the nonpolar and polar solvents (Table 2). Furthermore, no H-bond is observed in the prereaction complexes with $^•CH_2OH$, decreasing the stability and implying a much less favorable scavenging event.

As expected, the reaction with the $^•OH$ free radicals is much faster than with the other free radicals (k^{PCET} = 6.3×10^6 and 2.9×10^7 M^{-1} s^{-1} in the nonpolar and polar solvents, respectively, Table 2). According to the quantitative underestimation of k by DFT, this process can clearly be considered diffusion-controlled, being almost barrierless.

3.2. Electron-Transfer Processes (ET-PT and SPLET). Though PCET from a given OH group can only take place when the corresponding [**HBi**]-type prereaction complex is formed, ET can occur when either the [**HBi**]-type (complexes [**HB3**], [**HB3′**], [**HB4′**], [**HB5**], and [**HB7**] with the 3-OH, 3′-OH, 4′-OH, 5-OH, and 7-OH groups, respectively) or $[\nu-\pi]$-type (complexes $[\nu-\pi]_A$, $[\nu-\pi]_B$ and $[\nu-\pi]_C$, with the A-, B-, and C-rings, respectively) prereaction complexes are formed. The [**HBi**]-type prereaction complexes are globally more stable by about 2−3 kcal mol^{-1} than the $[\nu-\pi]$-type complexes (Tables 3 and 4).

Within the Marcus−Levich−Jortner formalism, the rate constant of the electron transfer (for the ET-PT and SPLET mechanisms) between the donor (quercetin) and the acceptor (the free radical) is expressed as[70]

dx.doi.org/10.1021/jp3116319 | J. Phys. Chem. A 2013, 117, 2082−2092

$$k^{\text{LJ-Marcus}} = \frac{4\pi^2}{h}\cdot V_{\text{RP}}{}^2\cdot\sqrt{\frac{1}{4\pi\lambda_s k_b T}} \times \sum_{\nu'}\left\{\exp(-S)\cdot\frac{S^{\nu'}}{\nu'!}\cdot\exp\left[-\frac{(\Delta G^\circ + \lambda_s + \nu'\hbar\langle\omega\rangle)^2}{4\lambda_s k_b T}\right]\right\} \quad (13)$$

where ΔG° is the Gibbs energy difference of reactions 2 or 5, λ_s the external reorganization energy, V_{RP} the electronic coupling, S the Huang–Rhys factor, and ν' is a vibrational quantum number.

ΔG° estimation has been made by considering the total Gibbs energies of the isolated species (reactants and products), neglecting the entropy effects for the electrostatic interaction between the species that are accounted by a classical Coulomb term:[71]

$$\Delta G^\circ = [G_{298\text{K}}(\text{ArOH}^{\bullet+}) + G_{298\text{K}}(\text{R}^-)] - [G_{298\text{K}}(\text{ArOH}) + G_{298\text{K}}(\text{R}^\bullet)] + E_{\text{Coulomb}} \quad \text{for ET-PT} \quad (14a)$$

$$\Delta G^\circ = [G_{298\text{K}}(\text{ArO}^\bullet) + G_{298\text{K}}(\text{R}^-)] - [G_{298\text{K}}(\text{ArO}^-) + G_{298\text{K}}(\text{R}^\bullet)] + E_{\text{Coulomb}} \quad \text{for SPLET} \quad (14b)$$

where $G_{298\text{K}}(\text{ArOH}^{\bullet+})$, $G_{298\text{K}}(\text{ArO}^\bullet)$, $G_{298\text{K}}(\text{ArO}^-)$, $G_{298\text{K}}(\text{R}^-)$, $G_{298\text{K}}(\text{ArOH})$, and $G_{298\text{K}}(\text{R}^\bullet)$ are the total free energies of the equilibrated isolated species $\text{ArOH}^{\bullet+}$, $\text{ArO}^\bullet$, ArO^-, R^-, ArOH, and $\text{R}^\bullet$, respectively.

Electron transfer is a multipath process because in principle the electron can be transferred from each MO (molecular orbital) of quercetin having an energy higher than that of the SOMO (singly occupied molecular orbital) of the free radical (Scheme 1). For quercetin, the MO involved in this electron transfer (to SOMO of the free radical) belongs to {HOMO–HOMO–n}, with n ranging from 1 to 8 depending on the radical (Supporting Information). The rate constant of each (HOMO–n)-to-SOMO path was calculated using eq 13. As the energies included in this equation refer to ground-state energies, ΔG° was corrected when HOMO–n differed from HOMO; it was corrected by the energy difference between HOMO and the corresponding HOMO–n levels. This MO energy difference was calculated with HF/Def2-TZVPP quality. Various levels of theories (DFT and HF with different basis sets) were used to evaluate this difference, but they provided similar trends (even if the absolute MO-energy values would require the use of high quantum level methods, the relative energies are much less method-dependent; see Supporting Information). The term E_{Coulomb} is defined as the difference in electrostatic interactions between reactants and products, calculated in first approximation in the geometries of the prereaction complexes.

Scheme 1. Molecular Orbital Diagram Showing Three Different Possible (HOMO–n)-to-SOMO Paths Corresponding to the Electron Transfer from Polyphenol Antioxidant to Free Radical[a]

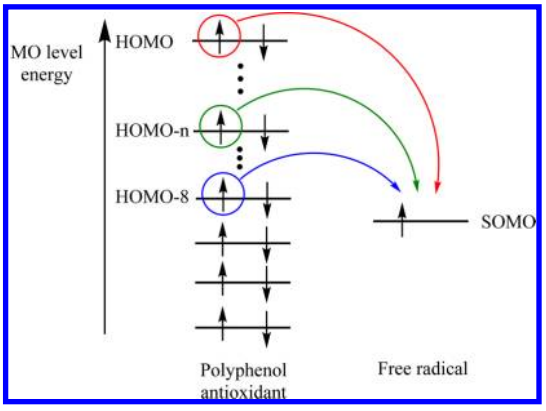

[a]In the case of quercetin, n ranges from 0 to 8 (corresponding MO energies being higher than SOMO).

$$E_{\text{Coulomb}} = \frac{1}{4\pi\varepsilon_0\varepsilon_s}\left(\sum_i^{\text{ArOH}^{+\bullet}}\sum_j^{\text{R}^-}\frac{q_i q_i}{r_{ij}} - \sum_k^{\text{ArOH}}\sum_l^{\text{R}^\bullet}\frac{q_k q_l}{r_{kl}}\right) \quad \text{for ET-PT} \quad (15a)$$

$$E_{\text{Coulomb}} = \frac{1}{4\pi\varepsilon_0\varepsilon_s}\left(\sum_i^{\text{ArO}^\bullet}\sum_j^{\text{R}^-}\frac{q_i q_i}{r_{ij}} - \sum_k^{\text{ArO}^-}\sum_l^{\text{R}^\bullet}\frac{q_k q_l}{r_{kl}}\right) \quad \text{for SPLET} \quad (15b)$$

where q_i and q_j (q_k and q_l) are atomic charges on the donor and acceptor units, respectively, and r_{ij} (r_{kl}) is the interatomic distance after (before) ET. All atomic charges were obtained within the CHELPG formalism;[72] ε_s is the static dielectric constant.

ΔG° thus depends on both the nature of the solvent and prereaction complexes. In the polar solvent, ΔG° values are similar for the different complexes. On the other hand, in the nonpolar solvent, ΔG° and therefore $k^{\text{LJ-Marcus}}$ strongly depend on the different free radical approaches (Tables 3 and 4).

λ_s is the external reorganization energy (i.e., related to the electronic and nuclear polarization of the solvent), which can be expressed as[73]

$$\lambda_s = \frac{1}{8\pi\varepsilon_0}\left(\frac{1}{\varepsilon_{\text{opt}}} - \frac{1}{\varepsilon_s}\right)\left(\frac{1}{r_{\text{ArOH}}} + \frac{1}{r_{\text{R}^\bullet}} + 2\sum_i^{\text{ArOH}}\sum_j^{\text{R}^\bullet}\frac{\Delta q_i \Delta q_j}{r_{ij}}\right) \quad \text{for ET-PT} \quad (16a)$$

$$\lambda_s = \frac{1}{8\pi\varepsilon_0}\left(\frac{1}{\varepsilon_{\text{opt}}} - \frac{1}{\varepsilon_s}\right)\left(\frac{1}{r_{\text{ArO}^-}} + \frac{1}{r_{\text{R}^\bullet}} + 2\sum_i^{\text{ArO}^-}\sum_j^{\text{R}^\bullet}\frac{\Delta q_i \Delta q_j}{r_{ij}}\right) \quad \text{for SPLET} \quad (16b)$$

where ε_{opt} is the optical dielectric constant. Δq_i and Δq_j are the differences in atomic charges along the electron-transfer reaction for the donor (i.e., ArOH and ArO^- for ET-PT and SPLET, respectively) and the acceptor (i.e., the free radical $\text{R}^\bullet$), respectively. The radii (r_{ArO^-}, r_{ArOH} and $r_{\text{R}^\bullet}$) were calculated as

$$r_{\text{R}^\bullet} \text{ or } r_{\text{ArOH}} \text{ or } r_{\text{ArO}^-} = \frac{1}{N}\sum_A^N |r_A - r_q| \quad (17)$$

where the sum runs over all atoms, r_A is the atomic position, and r_q is the charge-weighted barycenter of the molecule. This definition allows using a radius that is averaged according to its electrostatic significance.

The electronic coupling V_{RP} is estimated at the semiempirical Hartree–Fock intermediate neglect of differential overlap

dx.doi.org/10.1021/jp3116319 | J. Phys. Chem. A 2013, 117, 2082–2092

(INDO) level.[74] The electronic coupling term has been directly calculated between MOs of quercetin and the SOMO of the free radical, in the geometry of the prereaction complexes.[71] The coupling V_{ij} between two orbitals ϕ_i and ϕ_j (belonging to molecules i and j, respectively) can be classically recast in an atomic orbital basis set (eq 18):

$$V_{ij} = \langle \phi_i | h | \phi_j \rangle = \sum_{\mu} \sum_{\nu} c_{i\mu} c_{j\nu} \langle \chi_i | h | \chi_j \rangle \tag{18}$$

where $c_{i\mu}$ and $c_{j\nu}$ are the LCAO (linear combination of atomic orbitals) coefficients of the atomic orbitals χ_μ and χ_ν in the molecular orbitals ϕ_i and ϕ_j, respectively. In our case the coupling is calculated for each path, i.e., for each electron transition from all the HOMO−n having an energy higher than that of the SOMO of the free radical.[75] It must be stressed that MO shapes are very similar at both the INDO and DFT levels of calculation.

In eq 13 the summation runs over all vibrational levels of the effective mode, which represents in our case the aromatic C−C and phenolic C−O bond stretchings; the elongation of these bonds is the most probable reaction coordinate involved during the electron transfer. The corresponding energy is taken as their average energy ($\langle \hbar\omega \rangle$ = 4.6 kcal mol^{-1}). The Huang−Rhys factor S is directly related to the internal reorganization energy λ_i (i.e., the geometry reorganization along the reaction coordinate[76]):

$$S = \frac{\lambda_i}{\hbar\omega} \tag{19}$$

The global rate constant is the sum of the rate constants calculated for each accessible pathway. Even though many pathways exhibit large electronic couplings, the electron transfer is mainly dominated by the HOMO to SOMO pathway. When the electron is transferred from HOMO−n rather than from HOMO, the large increase in ΔG° makes the pathways really unlikely.

The robustness of such an application of Marcus theory has been largely shown for various systems.[71,76]

3.2.1. ET-PT: Pure Electron Transfer. Whatever the prereaction complex, the calculated rate constants of ET between quercetin and $CH_3OO^\bullet$ radicals are very small, lower than 10^{-100} M^{-1} s^{-1} in the nonpolar solvent (Table 3a). This definitely makes this process unfeasible in such an environment. Such extremely low rate constants are attributed to the high instability of the $ArOH^{\bullet+}$ radical cation in nonpolar solvents. Moreover, due to the large positive value of ΔG°, tunneling is not an efficient physical event that could compensate for the height of the activation barrier. Polar solvent induces a dramatic increase in the radical cation stability (Table 3b); ΔG^{ET} is 29.0 kcal mol^{-1} but the corresponding rate constants are still very low ($k^{ET\text{-}PT}$ ranging from 10^{-14} to 10^{-59} M^{-1} s^{-1}, Table 3b).

The ET step is followed by PT (reaction 3). This reaction is very exothermic (ΔG^{PT} lower than −25 and −70 kcal mol^{-1} in the polar and nonpolar solvent, respectively). Nonetheless, ET exhibits too low rate constants, whatever the solvent polarity, making the whole process totally inefficient in both hydrophilic and lipophilic environments.

The ET-PT process with $^\bullet CH_2OH$ is even slower than with $CH_3OO^\bullet$ ($k^{ET\text{-}PT}$ lower than 10^{-100} M^{-1} s^{-1} in both the polar and nonpolar solvents, Table 3). Such low values are again attributed not only to the high instability of the radical cation but also to the higher instability of $^-CH_2OH$ with respect to CH_3OO^-, due to a reduced charge delocalization: the charge is around −1.72 |e| on the C-atom of $^-CH_2OH$ vs −0.75 |e| on the O-atom of CH_3OO^-.

Electron transfer to the $CH_3O^\bullet$ free radical is still not competitive as compared to PCET in the nonpolar solvent ($k^{ET\text{-}PT}$ is very low, Table 3).

In the specific case of the $^\bullet OH$ free radical, no prereaction complex was obtained with DFT-D calculations. This indicates that for this very reactive free radical, it is impossible to distinguish between the ET-PT and PCET processes.

3.2.2. SPLET: An Activated Electron-Transfer Process. In SPLET, the electron transfer occurs from a deprotonated form of quercetin (eq 5). It means that the initiation of this mechanism strongly depends on pH of the medium and the acidity of the different OH groups of quercetin. It is known that the pH influences the antioxidant activity: the higher the pH, the higher the free radical scavenging activity of various polyphenols (e.g., flavonoids and curcuminoids).[26,67,77,78] From the relative Gibbs energies of stabilization of the different deprotonated forms according to eq 4 (Table 5), the 7-OH group appears to be the most acidic site and the following hierarchy is obtained 7-OH > 4′-OH > 3-OH > 5-OH > 3′-OH. This confirms the experimental pK_A values of 7.7, 8.8, 9.8 and 5.7, 7.1, and 8.0 (in methanol and water, respectively) obtained for the three most acidic groups: 7-OH, 4′-OH, and 3-OH, respectively.[67,79] The deprotonation is naturally very unfavorable in nonpolar solvents due to the ionic nature of the products, which cannot be stabilized. Therefore, the SPLET process cannot occur in nonpolar environments and under acidic conditions (e.g., digestive tract).

Table 5. Relative Gibbs energies ΔG (kcal mol^{-1}) for the Different Depronated Forms of Quercetin in the Polar Solvent

anion	3-OH	3′-OH	4′-OH	5-OH	7-OH
ΔG	4.1	6.8	3.2	5.0	0.0

The electron transfer occurs after the formation of the prereaction complex, in which quercetin is deprotonated; i.e., H^+ is released from one of the most acidic groups 7-OH, 4′-OH, or 3-OH. The rate constants were calculated for all prereaction complexes formed with quercetin deprotonated at 7-OH (complexes [**HB3**]-7H+, [**HB3′**]-7H+, [**HB4′**]-7H+, [**HB5**]-7H+, and all [$\nu-\pi$]-7H+) and with three other prereaction complexes with quercetin deprotonated at 4′-OH and 3-OH (complexes [**HB7**]-4′H+, [**HB7**]-3H+, and [**HB3′**]-3H$^+$) (Table 4).

One of the major results gained by quantum-chemical calculations is that rate constants strongly depend on both the prereaction complex and the site of deprotonation. For $CH_3OO^\bullet$-scavenging by quercetin, the rate constants range from 10^{-9} to 10^{7} M^{-1} s^{-1}. When quercetin is deprotonated at 7-OH, the highest rate constant is obtained with the prereaction complex [**HB4′**]-7H+ (k^{SPLET} is 4.0×10^{-1} M^{-1} s^{-1}, Table 4). When quercetin is deprotonated at 3-OH or 4′-OH, high rate constants are observed, e.g., k^{SPLET} is 1.3×10^{7} M^{-1} s^{-1} for the [**HB3′**]-3H+ prereaction complex (Table 4). The deprotonation induces a decrease in the polyphenol stability, which somewhat activates the electron-transfer process, which then becomes highly competitive with respect to PCET.

The SPLET reaction with $^\bullet CH_2OH$ appears to be totally inefficient in both nonpolar and polar environments. The rate constant in the polar solvent is around 10^{-52} M^{-1} s^{-1} (Table 4). This very low value is partly attributed to the poor stability of the

dx.doi.org/10.1021/jp3116319 | J. Phys. Chem. A 2013, 117, 2082−2092

products formed after electron transfer: (ΔG° = 49.0 kcal mol^{-1}, Table 4). In this case, the rate constant is further strongly affected by the internal reorganization energy (λ_i = 20.5 kcal mol^{-1}) when going from the $^\bullet CH_2OH$ free radical to the $^-CH_2OH$ anion, due to the hybridization change of the C-atom from sp^2 to sp^3.

SPLET with the alkoxyl radicals is also an activated-ET process. The rate constants increase from 2.3 × 10^{-12} to 2.3 × 10^{12} M^{-1} s^{-1} going from ET-PT to SPLET (Tables 3 and 4). In the polar solvent, SPLET is faster than PCET (Tables 2 and 4), making SPLET the most likely process to scavenge alkoxyl free radicals in polar solvents in a diffusion-controlled regime.

In the case of the $^\bullet OH$ free-radical, no prereaction complex was obtained at the theoretical level. A barrierless reaction is suspected because the electron transfer systematically occurs from all starting geometries for these complexes. This radical is highly reactive and, whatever the mechanism of action (PCET, ET-PT, or SPLET), its scavenging is diffusion-controlled.

4. CONCLUDING REMARKS

Whatever the polarity of the solvent, ET-PT is totally inefficient due to the high instability of the ArOH$^{\bullet+}$ radical cation, except for the specific case of the $^\bullet OH$ free-radical.

In nonpolar environments (e.g., lipid bilayer membranes), PCET is the only active process because the deprotonation of quercetin is highly unlikely, making SPLET infeasible. In other words, PCET is the major process able to break the chain reaction in lipid peroxidation, i.e., LOO$^\bullet$ free radical scavenging inside the membrane. At low pH (e.g., in the stomach), PCET is also the only possible process.

In polar solvents, e.g., in plasma, the pH ranges from 7.35 to 7.45, so that quercetin is partially deprotonated. Both PCET (from the neutral form) and SPLET (from the deprotonated form) are in competition, the latter appearing as the fastest and hence as the dominant process in agreement with the literature[36] (Tables 2b and 4). Nonetheless, an important point highlighted in the present work is that this competition strongly depends on the prereaction complex and the deprotonation site. From a statistical point of view, SPLET offers much more possibilities because the number of complexes-of-approach with free radicals associated with high rate constants is higher with SPLET than with PCET. For an effective scavenging by H-atom abstraction, the free radicals should approach (i) all OH groups and the aromatic rings to form $\nu-\pi$ complexes (e.g., $[\nu-\pi]_C$) with SPLET or (ii) only the OH groups with a low BDE (i.e., 3-OH, 3′-OH, and 4′-OH) with PCET.

The competition also depends on the pH: the higher the pH, the higher the number of deprotonated sites and the higher the contribution of SPLET (yielding high to very high rate constants). This is in good agreement with the increase in the free radical scavenging with the pH experimentally observed for flavonoids.[26,67,77] As previously suggested from experimental studies under nonacidic conditions, SPLET is the fastest and major mechanism and PCET is slower and minor, modifying the kinetic regime.[36] This picture, involving both mechanisms, is probably the most adapted to rationalize scavenging of peroxyl radicals (and also DPPH radicals that have shown a similar behavior[36] and are widely used in antioxidant evaluations). For free radical scavenging of carbon-centered and alkoxyl radicals, the major process is PCET and SPLET, respectively. To scavenge $^\bullet OH$ free radicals, both mechanisms are diffusion-controlled.

These conclusions are drawn out for quercetin, which is a relevant model of antioxidant highly representative of flavonoids. However, it must be stressed that these results can easily be extrapolated to a large class of compounds including other natural polyphenols, bioavailable metabolites, and new hemisynthetic derivatives. Quantum chemistry is shown here as a powerful tool to rationalize structure antioxidant activity relationships for both thermodynamic and kinetic aspects. In this way, this tool appears as very promising to support experimental expertise in food chemistry, cosmetology, and pharmaceutical applications. Even if the evaluation of k^{SPLET} appears quantitatively accurate, that of k^{PCET} requires further methodological developments to reach accuracy for a broad class of antioxidants.

■ ASSOCIATED CONTENT

Supporting Information

Thermodynamics of HAT between quercetin and the $CH_3OO^\bullet$ radical. Discussion on kinetic solvent effects (KSE). Energy difference between the highest occupied molecular orbitals of neutral and deprotonated quercetin and various radicals. This material is available free of charge via the Internet at http://pubs.acs.org.

■ AUTHOR INFORMATION

Corresponding Author

*Tel: +33 (0) 555 435 927. Fax: +33 (0) 555 435 845. E-mail: patrick.trouillas@unilim.fr.

Notes

The authors declare no competing financial interest.

■ ACKNOWLEDGMENTS

The authors thank the “Conseil Régional du Limousin” for financial support and CALI (CAlcul en LImousin) and IDRIS (Institut du Développement et des Ressources Informatiques Scientifiques, Orsay - Paris) for computing facilities. Research in Limoges is also supported by the COST action CM0804 “Chemical Biology with Natural Compounds”. The Mons-Limoges collaboration is supported by FNRS. Research in Mons is also supported by the Belgian Federal Government Science Policy Office (PAI 6/27), Région Wallonne (OPTI2MAT Excellence program) and FNRS-FRFC. J.C. is an FNRS Research Director. The authors gratefully acknowledge the support by the Operational Program Research and Development for Innovations−European Regional Development Fund (project CZ.1.05/2.1.00/03.0058 of the Ministry of Education, Youth and Sports of the Czech Republic).

■ REFERENCES

(1) Hertog, M. G.; Feskens, E. J.; Hollman, P. C.; Katan, M. B.; Kromhout, D. *Lancet* **1993**, *342*, 1007−11.
(2) Blake, D. R.; Allen, R. E.; Lunec, J. *Br. Med. Bull.* **1987**, *43*, 371−85.
(3) Commenges, D.; Scotet, V.; Renaud, S.; Jacqmin-Gadda, H.; Barberger-Gateau, P.; Dartigues, J. F. *Eur. J. Epidemiol.* **2000**, *16*, 357−363.
(4) Boots Agnes, W.; Li, H.; Schins Roel, P. F.; Duffin, R.; Heemskerk Johan, W. M.; Bast, A.; Haenen Guido, R. M. M. *Toxicol. Appl. Pharmacol.* **2007**, *222*, 89−96.
(5) Saller, R.; Meier, R.; Brignoli, R. *Drugs* **2001**, *61*, 2035−2063.
(6) Gazak, R.; Marhol, P.; Purchartova, K.; Monti, D.; Biedermann, D.; Riva, S.; Cvak, L.; Kren, V. *Process Biochem.* **2010**, *45*, 1657−1663.
(7) Rice-Evans, C. A.; Van Acker, S. A. B. *Flavonoids in health and disease*; Marcel Dekker: New York, 1998.
(8) Rice-Evans, C.; Miller, N. J.; Paganga, G. *Free Radical Biol. Med.* **1996**, *20*, 933−956.

(9) Cos, P.; Ying, L.; Calomme, M.; Hu, J. P.; Cimanga, K.; Van Poel, B.; Pieters, L.; Vlietinck, A. J.; Vanden Berghe, D. *J. Nat. Prod.* **1998**, *61*, 71−76.
(10) Trouillas, P.; Marsal, P.; Siri, D.; Lazzaroni, R.; Duroux, J.-L. *Food Chem.* **2006**, *97*, 679−688.
(11) Kozlowski, D.; Trouillas, P.; Calliste, C.; Marsal, P.; Lazzaroni, R.; Duroux, J.-L. *J. Phys. Chem. A* **2007**, *111*, 1138−1145.
(12) Trouillas, P.; Marsal, P.; Svobodova, A.; Vostalova, J.; Gazak, R.; Hrbac, J.; Sedmera, P.; Kren, V.; Lazzaroni, R.; Duroux, J.-L.; et al. *J. Phys. Chem. A* **2008**, *112*, 1054−1063.
(13) Anouar, E.; Calliste, C. A.; Kosinova, P.; Di Meo, F.; Duroux, J. L.; Champavier, Y.; Marakchi, K.; Trouillas, P. *J. Phys. Chem. A* **2009**, *113*, 13881−13891.
(14) Leopoldini, M.; Pitarch, I. P.; Russo, N.; Toscano, M. *J. Phys. Chem. A* **2004**, *108*, 92−96.
(15) Leopoldini, M.; Marino, T.; Russo, N.; Toscano, M. *Theor. Chem. Acc.* **2004**, *111*, 210−216.
(16) Lucarini, M.; Pedulli, G. F.; Guerra, M. *Chem.—Eur. J.* **2004**, *10*, 933−939.
(17) Priyadarsini, K. I.; Maity, D. K.; Naik, G. H.; Kumar, M. S.; Unnikrishnan, M. K.; Satav, J. G.; Mohan, H. *Free Radical Biol. Med.* **2003**, *35*, 475−484.
(18) Fiorucci, S.; Golebiowski, J.; Cabrol-Bass, D.; Antonczak, S. *J. Agric. Food Chem.* **2007**, *55*, 903−911.
(19) Fiorucci, S.; Golebiowski, J.; Cabrol-Bass, D.; Antonczak, S. *ChemPhysChem* **2004**, *5*, 1726−1733.
(20) Russo, N.; Toscano, M.; Uccella, N. *J. Agric. Food Chem.* **2000**, *48*, 3232−3237.
(21) Kong, L.; Wang, L.-F.; Zhang, H.-Y. *J. Mol. Struct. THEOCHEM* **2005**, *716*, 27−31.
(22) Foti, M. C.; Daquino, C.; Mackie, I. D.; DiLabio, G. A.; Ingold, K. U. *J. Org. Chem.* **2008**, *73*, 9270−9282.
(23) Foti, M. C.; Daquino, C.; Geraci, C. *J. Org. Chem.* **2004**, *69*, 2309−2314.
(24) A detailed analysis of the thermodynamic aspects of the HAT-type reaction between the flavonoid quercetin (Figure 1a) and ROO$^{\bullet}$ radicals is presented in the Supporting Information.
(25) Leopoldini, M.; Marino, T.; Russo, N.; Toscano, M. *J. Phys. Chem. A* **2004**, *108*, 4916−4922.
(26) Litwinienko, G.; Ingold, K. U. *J. Org. Chem.* **2003**, *68*, 3433−8.
(27) De Heer, M. I.; Mulder, P.; Korth, H.-G.; Ingold, K. U.; Lusztyk, J. *J. Am. Chem. Soc.* **2000**, *122*, 2355−2360.
(28) Snelgrove, D. W.; Lusztyk, J.; Banks, J. T.; Mulder, P.; Ingold, K. U. *J. Am. Chem. Soc.* **2001**, *123*, 469−477.
(29) MacFaul, P. A.; Ingold, K. U.; Lusztyk, J. *J. Org. Chem.* **1996**, *61*, 1316−1321.
(30) Foti, M. C.; Amorati, R.; Pedulli, G. F.; Daquino, C.; Pratt, D. A.; Ingold, K. U. *J. Org. Chem.* **2010**, *75*, 4434−4440.
(31) DiLabio, G. A.; Johnson, E. R. *J. Am. Chem. Soc.* **2007**, *129*, 6199−6203.
(32) Lingwood, M.; Hammond, J. R.; Hrovat, D. A.; Mayer, J. M.; Borden, W. T. *J. Chem. Theo. Comput.* **2006**, *2*, 740−745.
(33) Hatcher, E.; Soudackov, A. V.; Hammes-Schiffer, S. *J. Am. Chem. Soc.* **2006**, *129*, 187−196.
(34) Hammes-Schiffer, S. *Energy Environ. Sci.* **2012**, *5*, 7696−7703.
(35) Burton, G. W.; Doba, T.; Gabe, E.; Hughes, L.; Lee, F. L.; Prasad, L.; Ingold, K. U. *J. Am. Chem. Soc.* **1985**, *107*, 7053−65.
(36) Litwinienko, G.; Ingold, K. U. *Acc. Chem. Res.* **2007**, *40*, 222−230.
(37) K. M. Mayer recently proposes to use the same terminology (HAT), which makes sense in a global quantum picture.
(38) Jovanovic, S. V.; Steenken, S.; Tosic, M.; Marjanovic, B.; Simic, M. G. *J. Am. Chem. Soc.* **1994**, *116*, 4846−51.
(39) Jovanovic, S. V.; Steenken, S.; Hara, Y.; Simic, M. G. *J. Chem. Soc., Perkin Trans. 2* **1996**, 2497−2504.
(40) Zhang, H.-Y.; Ji, H.-F. *New J. Chem.* **2006**, *30*, 503−504.
(41) Brede, O.; Ganapathi, M. R.; Naumov, S.; Naumann, W.; Hermann, R. *J. Phys. Chem. A* **2001**, *105*, 3757−3764.
(42) Galati, G.; O'Brien, P. J. *Free Radical Biol. Med.* **2004**, *37*, 287−303.
(43) Crozier, A.; Del Rio, D.; Clifford, M. N. *Mol. Asp. Med.* **2010**, *31*, 446−467.
(44) Goupy, P.; Vulcain, E.; Caris-Veyrat, C.; Dangles, O. *Free Radical Biol. Med.* **2007**, *43*, 933−946.
(45) Roche, M.; Dufour, C.; Mora, N.; Dangles, O. *Org. Biomol. Chem.* **2005**, *3*, 423−430.
(46) Vulcain, E.; Goupy, P.; Caris-Veyrat, C.; Dangles, O. *Free Rad. Res.* **2005**, *39*, 547−563.
(47) Sánchez-Moreno, C.; A. Larrauri, J.; Saura-Calixto, F. *Food Res. Int.* **1999**, *32*, 407−412.
(48) Carbon centered free radicals are radical intermediates produced by HAT from the lipid chains, prior to dioxygen addition, during the lipid peroxidation process. They are also produced, e.g., in liver intoxication to alcohol.
(49) Feng, Y.; Liu, L.; Wang, J.-T.; Huang, H.; Guo, Q.-X. *J. Chem. Inf. Comput. Sci.* **2003**, *43*, 2005−2013.
(50) Kosinova, P.; Di Meo, F.; Anouar, E. H.; Duroux, J.-L.; Trouillas, P. *Int. J. Quantum Chem.* **2011**, *111*, 1131−1142.
(51) Anouar, E.; Kosinova, P.; Kozlowski, D.; Mokrini, R.; Duroux, J. L.; Trouillas, P. *Phys. Chem. Chem. Phys.* **2009**, *11*, 7659−7668.
(52) Grimme, S. *J. Comput. Chem.* **2004**, *25*, 1463−1473.
(53) Di Meo, F.; Sancho Garcia, J. C.; Dangles, O.; Trouillas, P. *J. Chem. Theo. Comput.* **2012**, *8*, 2034−2043.
(54) Frisch, M. J.; Trucks, G. W.; Schlegel, H. B.; Scuseria, G. E.; Robb, M. A.; Cheeseman, J. R.; Scalmani, G.; Barone, V.; Mennucci, B.; Petersson, G. A.; et al. *Gaussian 09*, Revision A.02; Gaussian, Inc.: Wallingford, CT, 2009.
(55) Zhao, Y.; Truhlar, D. G. *J. Phys. Chem. A* **2004**, *108*, 6908−6918.
(56) We have checked that the thermodynamics are similar for both (U)B3P86/6-31+G(d,p) and (U)MPWB1K/6-31+(d,p).
(57) Cossi, M.; Scalmani, G.; Rega, N.; Barone, V. *J. Chem. Phys.* **2002**, *117*, 43−54.
(58) Tomasi, J.; Mennucci, B.; Cammi, R. *Chem. Rev.* **2005**, *105*, 2999−3093.
(59) Neese, F. *WIREs Comput. Mol. Sci.* **2012**, *2*, 73−78.
(60) Chiodo, S. G.; Leopoldini, M.; Russo, N.; Toscano, M. *Phys. Chem. Chem. Phys.* **2010**, *12*, 7662−7670.
(61) Eyring, H. *J. Chem. Phys.* **1935**, *3*, 107−115.
(62) Truhlar, D. G.; Hase, W. L.; Hynes, J. T. *J. Phys. Chem.* **1983**, *87*, 2664−2682.
(63) Skodje, R. T.; Truhlar, D. G. *J. Phys. Chem.* **1981**, *85*, 624−8.
(64) Tejero, I.; González-García, N.; González-Lafont, À.; Lluch, J. M. *J. Am. Chem. Soc.* **2007**, *129*, 5846−5854.
(65) This process has recently been studied for the scavenging reaction between quercetin and $CH_3OO^{\bullet}$ (see ref 60). Here we reproduced the calculation with this free radical, as our methodology slightly differs from the methodology used in this publication. As seen in this section, results obtained with both methodologies are similar; however, these new calculations are mandatory to ensure consistency throughout the text (all other sections) and to allow comparisons (i) between the different free radicals and (ii) between the atom-transfer and electron-transfer processes.
(66) Butković, V.; Klasinc, L.; Bors, W. *J. Agric. Food Chem.* **2004**, *52*, 2816−2820.
(67) Musialik, M.; Kuzmicz, R.; Pawlowski Tomasz, S.; Litwinienko, G. *J. Org. Chem.* **2009**, *74*, 2699−709.
(68) Belyakov, V. A.; Roginsky, V. A.; Bors, W. *J. Chem. Soc., Perkin Trans. 2* **1995**, 2319−2326.
(69) Abraham, M. H.; Grellier, P. L.; Prior, D. V.; Morris, J. J.; Taylor, P. J. *J. Chem. Soc., Perkin Trans. 2* **1990**, 521−9.
(70) Bixon, M.; Jortner, J. *Electron Transfer—from Isolated Molecules to Biomolecules*; John Wiley & Sons, Inc.: New York, 2007; pp 35−202.
(71) Van Vooren, A.; Lemaur, V.; Ye, A.; Beljonne, D.; Cornil, J. *ChemPhysChem* **2007**, *8*, 1240−1249.
(72) Breneman, C. M.; Wiberg, K. B. *J. Comput. Chem.* **1990**, *11*, 361−373.
(73) Marcus, R. A. *J. Chem. Phys.* **1965**, *43*, 679−701.
(74) Ridley, J.; Zerner, M. *Theor. Chem. Acc.* **1973**, *32*, 111−134.

(75) The electronic coupling term V_{RP} does not strongly depend on the nature of the complexes except for [**HB7**] and $[\nu-\pi]_C$ due to the strong electronic coupling between HOMO−2 and the SOMO (Table 4). Electronic coupling does not depend on the solvent because the geometries of the complexes are very similar with both nonpolar and polar solvents.
(76) Lemaur, V.; Steel, M.; Beljonne, D.; Bredas, J.-L.; Cornil, J. *J. Am. Chem. Soc.* **2005**, *127*, 6077−6086.
(77) Galano, A.; Alvarez-Diduk, R.; Ramirez-Silva, M. T.; Alarcon-Angeles, G.; Rojas-Hernandez, A. *Chem. Phys.* **2009**, *363*, 13−23.
(78) Musialik, M.; Litwinienko, G. *Org. Lett.* **2005**, *7*, 4951−4954.
(79) Escandar, G. M.; Sala, L. F. *Can. J. Chem.* **1991**, *69*, 1994−2001.